INTEGRATION OF CYGNSS WIND AND WAVE OBSERVATIONS WITH THE WAVEWATCH III NUMERICAL MODEL

Tianlin Wang[1], Valery U. Zavorotny[2, 3], Joel Johnson[4], Yuchan Yi[5], Christopher Ruf[1]

[1]University of Michigan, Ann Arbor, MI USA
[2] Cooperative Inst. for Research in Environmental Sciences, University of Colorado, Boulder, CO USA
[3]NOAA Earth System Research Laboratory, Physical Sciences Division, Boulder, CO USA
[4]ElectroScience Laboratory, The Ohio State University, Columbus, OH USA
[5]School of Earth Sciences, The Ohio State University, Columbus, OH USA

ABSTRACT

The Cyclone Global Navigation Satellite System (CYGNSS) mission employs measurements of the quasi-specular forward scattering cross section of the ocean surface for retrieving sea surface wind speed and roughness globally and, particularly, in the inner core of tropical cyclones. CYGNSS Level 2 data products include the ocean surface wind speed U_{10} and the mean square slope (MSS). An "excess MSS" approach has been previously proposed to account for sea state condition effects, including the presence of non-local swell and the degree of wave development, to reduce the influence of these effects and thereby improve wind speed retrievals. The approach requires ancillary information on the sea surface MSS and wind speed from models, and has been shown to provide some improvement in wind speed retrievals. In this work, the inclusion of an additional parameter, the inverse wave age, is examined to determine if additional improvements can be achieved. MSS and inverse wave age information is obtained from the WaveWatch III model run by IFREMER, and is used to compute a feedback signal for a closed-loop retrieval algorithm for both wind speed and MSS. The goal of the effort is to improve further the accuracy of CYGNSS Level 2 wind speed retrievals, and also to provide additional wave information if possible. This paper also investigates the technical methodology and potential benefits of integrating CYGNSS observations into the WW3 model.

Index Terms— CYGNSS, inverse wave age, mean square slope (MSS), sea state, WaveWatch III, wind speed

1. INTRODUCTION

The Cyclone Global Navigation Satellite System (CYGNSS) mission measures ocean surface roughness and wind speed [1]. The current baseline Level 2 retrieval algorithm for the wind speed is an empirical approach based on the use of "ground truth" winds (from the ECMWF model) and CYGNSS observables [2]. There are two types of geophysical modeling function (GMF), developed for the wind speed retrieval at different sea states, called the "fully developed seas" and "young seas limited-fetch" cases. However, this division oversimplifies the large variety of sea state behaviors and does not account for the presence of non-local swell.

It has also been demonstrated that the error of wind speeds retrieved from GNSS-Reflectometry (GNSS-R) observations is strongly correlated with the significant wave height (SWH) of the ocean [3]. Hence there is a necessity to take into account the sea state influence, especially the non-local swell contribution to the ocean surface roughness.

An "excess MSS" approach for improving CYGNSS wind speed retrieval was proposed in [4] to address these issues. The approach computes the "excess MSS", responsible for sea-state development effects, as the difference between the MSS from the IFREMER (Institut Francais de Recherche pour l'Exploitation de la MER) implementation of the WaveWatch III (WW3) numerical model [5] and the "local MSS" calculated using a version of the Elfouhaily et al. spectral model [6]. After subtracting the excess MSS term from the CYGNSS measured MSS, the local wind portion of the CYGNSS MSS is generated and can be used for higher accuracy wind speed retrieval. Note that use of the "excess MSS" should have a limited correlation with the model winds forcing the WW3 predictions since the approach attempts to remove local wind contributions to the MSS.

Based on a large-scale analysis of 200 days' data, it has been demonstrated that at relatively low wind speed (U_{10} less than 15 m/s): 1) the computed excess MSS has approximately a 50 % correlation with the significant wave height (SWH), since the latter term is dominated by the swell rather than the local wind; 2) the excess MSS approach reduces the correlation between wind speed retrieval error with the SWH [7]. These results demonstrate that the excess MSS reflects the contribution of non-local swell in low wind speed scenarios.

More recent analysis has shown that the IFERMER MSS has a dependence not only on the wind speed but also on wave age. Factoring wave age information into the excess MSS

approach and retrieval process is therefore considered in this work.

In the updated algorithm presented in this paper, an initial guess for the inverse wave age is derived from IFERMER WW3 products and then combined with the ground truth wind speed (ECMWF) to compute a modified "local MSS". Then a closed-loop algorithm is applied to iterate wind speed and inverse wave age estimates until consistency of the ocean surface wind speed retrieved between CYGNSS and WW3 information.

2. BRIEF OVERVIEW OF EXCESS MSS APPROACH

The surface plot in Figure 1 gives an example of an energy density spectrum of the ocean waves at Christmas Island (NOAA buoy 51028) at 12:00 UTC on November 9, 2000 (adopted from the user manual of WAVEWATCH II [5]).

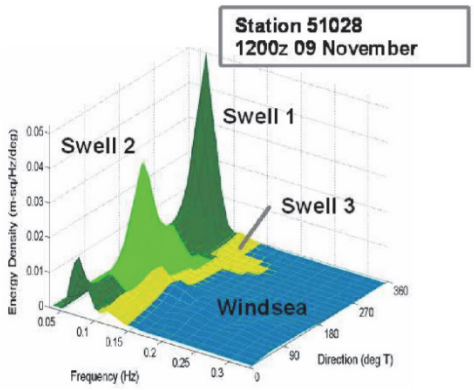


Figure. 1 Example of surface wave energy density spectrum

The spectrum shows four spectral partitions, including the area of the wind-sea and three swell trains. Obviously, the swell partition is more directional than the wind-sea partition. The swell partition typically has a narrower spectrum with a larger amplitude and its peak position in the low frequency (long wave) region, while the wind-sea partition has a wider spectrum with a smaller amplitude and its peak position in the high frequency (short wave) region. Such behavior is typical for wave spectra measured in the field. See, for example, the surface spectra reported in the Wind and Salinity Experiment (WISE) 2001 field campaign [8, 9].

Figure 2, using a one-dimensional version of the spectral density in Fig. 1, illustrates the basic physical principles for the excess MSS approach. The excess MSS is the difference between the WW3 MSS and the wind generated MSS as

$$\Delta\tilde{s}^2 = \tilde{s}^2_{WW} - \tilde{s}^2 \qquad (1)$$

where $\tilde{s}^2_{WW}$ is the WW3 MSS is produced from the wave spectrum $\Psi_{WW}(\vec{\kappa})$ and $\tilde{s}^2$ is the modeled MSS due to the local wind using the Elfouhaily *et al.* spectrum [6].

Then, by subtracting the excess MSS from the CYGNSS MSS, the wind dependent portion is calculated as

$$\tilde{s}^2_{CY} = s^2_{CY} - \Delta\tilde{s}^2 \qquad (2)$$

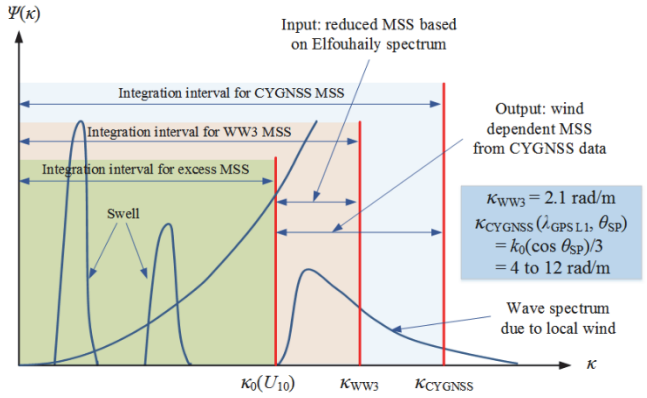


Figure. 2 Sketch illustrating basic principles of the excess MSS approach

The wind speed retrieval is then attempted by converting $\tilde{s}^2_{CY}$ back into a corrected NBRCS and performing a retrieval using the GMFs. More details are discussed in Section 5.

There is also another important parameter characterizing the waves, the inverse wave age Ω. An initial value for the inverse wave age Ω_0 for wind sea is estimated using the following equation

$$\Omega_0 = \frac{U_c}{c_{p0}} = \frac{2\pi U_{10}\cos\theta}{g T_{p0}} \qquad (3)$$

where θ is the angle between wave and wind directions, and T_{p0} is the wave period at the spectral peak for the wind-sea partition. Empirical models of ocean wave spectra predict that the inverse wave age Ω_0 of local wind seas at finite fetch are larger than the asymptotic value of 0.84 for infinite fetch [6]. The calculation of Ω_0 using wind speeds and wave periods T_{p0} from IFREMER WW3 data on average support this; however, a significant portion of realizations yield values of Ω_0 smaller than 0.84. This could be a result of wind gustiness and other complicated factors of wind-sea interaction.

In Section 3, analysis of the excess MSS demonstrates the necessity to consider both the non-local swells and the wave age information of the local wind sea. Not accounting for a limited fetch in the local wind sea might lead to a negative excess MSS values.

3. EXCESS MSS AND SEA STATE

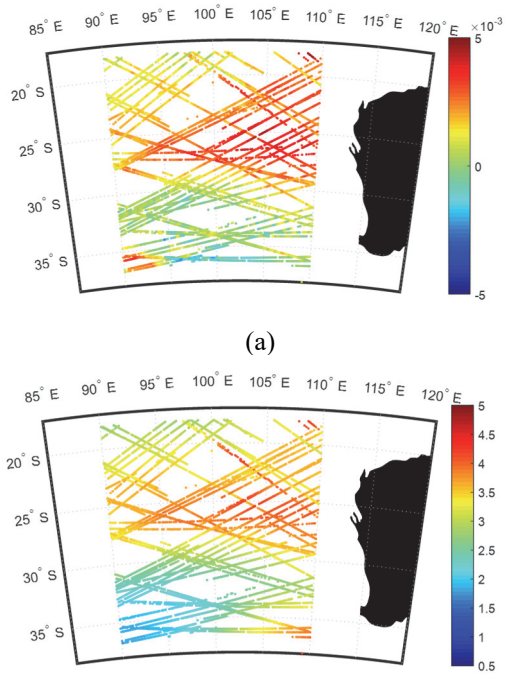
We use the wind and IFERMER MSS matchup data produced by our NOAA colleagues to analyze the relation between the excess MSS and other sea state parameters as shown below.

3.1 Positive excess MSS and SWH

On April 7th, 2018, two different sea states were present in the ocean close to the west coast of Australia.

Figure 3a shows the map of the calculated excess MSS assuming a fully-developed sea with inverse wave age Ω =

0.84 and Figure 3b shows the map of SWH. It shows a strong correlation: in the upper region, the positive excess MSS is related to the non-local swell, which also dominates the wave height at relatively low wind speed. In the lower region, the zero-mean excess MSS indicates that the effect of swell on the surface roughness is small because the swell wave is relatively weak, as shown in the SWH. This demonstrates that the positive excess MSS is due to the non-local swell, the result which we expected to see and which agrees with the physical insights in Section 2.



(a)

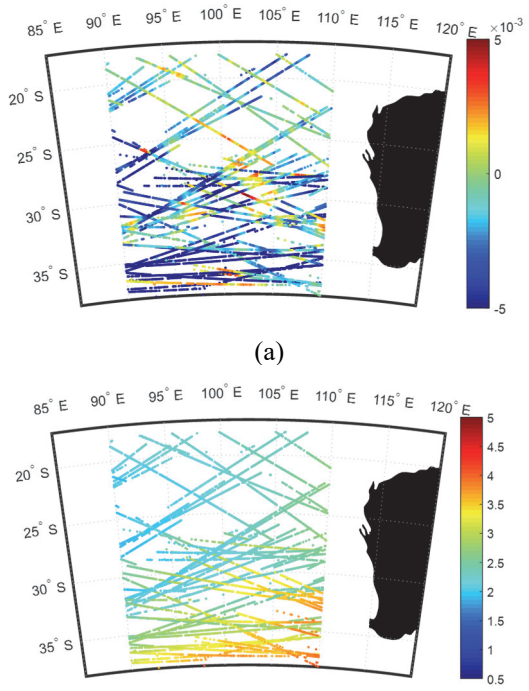
(b)

Figure. 3 Excess MSS and SWH on April 7th, 2018

3.2 Negative excess MSS and wave age

On April 17th, 2018, the sea state changes because there was a newly-generated cyclone in the southwestern corner of the area plotted in Figs 3 and 4. The seas are expected to be younger under such conditions. Figure 4a shows the map of the calculated excess MSS assuming a fully-developed sea with inverse wave age $\Omega = 0.84$, and Figure 4b shows the map of the SWH. It is interesting to notice that the excess MSS is negative for the lower region even with a relatively large SWH.

The explanation of such a behavior of the excess MSS is as follows. Even though swell makes positive contribution to the excess MSS, the second term of (1) is overestimated when using the fully-developed sea assumption. If the inverse wave age is greater than 0.84, which means a limited-fetch (young) sea, then the second term should be smaller than that for the fully-developed sea, as discussed in [4, 6].



(a)

(b)

Figure. 4 Excess MSS and SWH on April 17th, 2018

This demonstrates the effect of the wave development on the excess MSS approach and the necessity to include the inverse wave age into the analysis.

4. WW3 MSS DEPENDENCE ON WAVE AGE

We analyze the WW3 MSS and investigate the dependence on the wave age, as shown in Figure 5. The 3-hours' data points over the global ocean on May 1st, 2018 from 0000 to 0300 Z are binned for various intervals of the estimated inverse wave age. The corresponding MSS values are plotted versus the ECMWF wind speed in Figure 5. It shows that the wave age does affect the MSS: for instance, for fully developed sea with smaller Ω, the MSS is greater than that of the limited-fetch sea or young sea with much larger Ω. This behavior of the MSS is expected from the theoretical models of wind-generated ocean wave spectra [6].

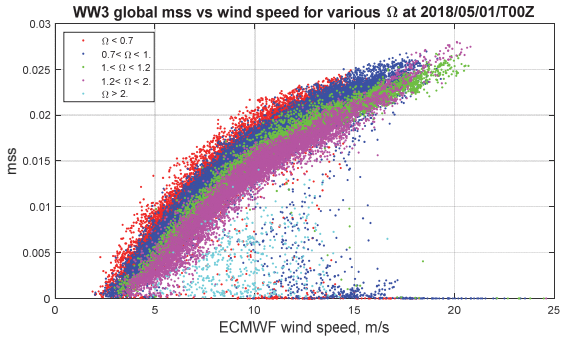


Figure. 5 WW3 MSS vs. wind speed for various Ω

Figure 6 shows a distribution of the global inverse wave age Ω_0 estimated using the global 3-hour WW3 data and relationship (3). The significant spread of Ω_0 also proves the necessity of inclusion the wave age information into the consideration.

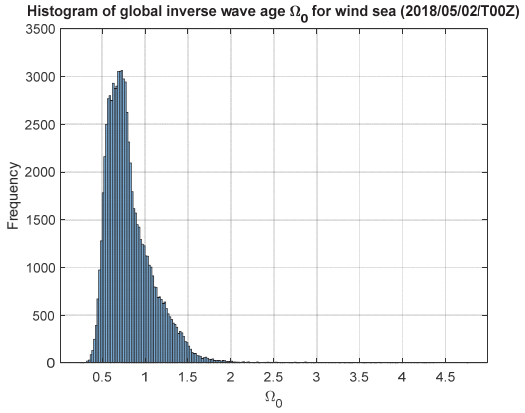


Figure. 6 Histogram of global inverse wave age

Initial attempts to analyze the dependence of CYGNSS MSS on the inverse wave age have been conducted. At present the results are inconclusive; further discussion will be provided in the conference presentation.

5. PROPOSED CLOSED-LOOP ALGORITHM

Because we have CYGNSS observations, we are also able to generate a feedback signal and develop a closed-loop algorithm by running the WW3 model and iterating the calculation of the excess MSS for better accuracy of sea state modeling and wind speed retrieval.

A conceptual process is described as follows: 1) the inverse wave age is initially obtained from WW3 wind sea partition data; 2) the wind speed and inverse wave age are the inputs to the Elfouhaily et al. spectrum [6] to compute the MSS of the wind sea; 3) the excess MSS is calculated by subtracting the wind sea modeled MSS from the WW3 MSS; 4) the wind dependent CYGNSS MSS is computed by subtracting the excess MSS from the raw measured MSS; 5) the inverse wave age is estimated using the wind sea CYGNSS MSS, wind speed and the specular incidence angle (dependent on the spectrum cutoff frequency); 6) the inverse wave age is compared with the initial value, and if they do not agree, then steps 2) to 6) are re-run until the two terms agree; 7) final data products are output using the new wave information and the wind dependent CYGNSS corrected MSS for wind speed retrieval.

This closed-loop algorithm takes the measurements by CYGNSS as additional constraints to the WW3 model, and invokes the use of ancillary wind speed information in order to focus on the retrieval of wave properties. The fast revisit measurements of the CYGNSS mission could then be a significant data source to improve the accuracy of the WW3 estimate.

6. SUMMARY AND DISCUSSION

In this paper, we report the recent progress of the excess MSS approach in [4] and its next phase of development to integrate CYGNSS ocean observations to the WW3 model.

We demonstrate that the excess MSS depends on the sea state which includes the non-local swell and wave age. By including these factors in our analysis, we can estimate the excess MSS more accurately which allows us to single out the wind-sea related MSS component from the original MSS measured by CYGNSS. By using a closed-loop algorithm with the inverse wave age and ancillary wind speed information as a control signal, enhanced wave estimates from CYGNSS may be possible.

The presented here approach does not account for an effect of the different wave directivities of swell partitions and wind sea in calculating of the excess MSS. Currently we are investigating the possibility of such an approach. More testing of the closed-loop algorithm is also in progress; results will be reported in the conference presentation.

7. REFERENCES

[1] C. S. Ruf, A. Lyons, M. Unwin, J. Dickinson, R. Rose, D. Rose, and M. Vincent, "CYGNSS: Enabling the future of hurricane prediction," *IEEE Geosci. Remote Sens. Mag.*, vol. 1, no. 2, pp. 52-67, June 2013.

[2] Ruf, C. S., et al., *CYGNSS Handbook*, Michigan Publishing, Ann Arbor, MI, 2016.

[3] M. P. Clarizia, C. S. Ruf, "Bayesian wind speed estimation conditioned on significant wave height for GNSS-R ocean observations," *J. Atmos. Ocean. Tech.*, vol. 34, no.6, pp.1193-1202, June 2017.

[4] T. Wang, V. U. Zavorotny, J. Johnson, C. Ruf and Y. Yi, "Modeling of sea state conditions for improvement of CYGNSS L2 wind speed retrievals," *Proc. IGARSS''18*, Valencia, pp. 8288-8291.

[5] WaveWatch III Development Group, "User manual and system documentation of WaveWatch III version 5.16," *MMAB Technical Note*, Oct. 2016.

[6] T. Elfouhaily, B. Chapron, and K. Katsaros, "A unified directional spectrum for long and short wind-driven waves," *J. Geophys. Res.*, vol. 102, no. C7, pp. 15781-15796, July 1997.

[7] T. Wang, V. U. Zavorotny, J. Johnson, C. Ruf and Y. Yi, "Investigation of ocean surface wind and wave coupling using CYGNSS observations," AGU 2018, Washington D.C., Dec. 2018.

[8] Camps, A. et al., "Wind and salinity experiment 2000 (WISE 2000): Sscientific analysis report," ESTEC Contract, Aug. 2001.

[9] J. Miranda, M. Vall-Ilossera, A. Camps, and N. Duffo, "Sea surface emissivity at L-band: Swell effects," *Proc. IGARSS'02*, vol.5, pp. 2623-2625, June 2002.